Contents lists available at ScienceDirect

Optik - International Journal for Light and Electron

journal homepage: www.elsevier.com

A novel filter wheel for multi-channel switching and polarization rotation

Chun-Jen Weng [a], Lijuan Wang [b], Chih-Yen Chen [c,*], Da-Ren Liu [a], Chi-Hung Hwang [a], Shian-Wen Chang [d]

[a] Taiwan Instrument Research Institute, National Applied Research Laboratories, 20, R&D Rd. VI, Hsinchu Science Park, Hsinchu, 30076 Taiwan, ROC
[b] School of Engineering and Digital Arts, University of Kent, Canterbury, Kent CT2 7NT, Room 1.21, Jennison Building, Canterbury, Kent, CT2 7NT, UK
[c] 39, St. Michaels Place, CT2 7HQ, UK
[d] National Synchrotron Radiation Research Center, No.101, Hsin-Ann Rd., Hsinchu Science Park, Hsinchu 30076, Taiwan, ROC

ARTICLE INFO

Keywords:
Filter wheel
Multi-channel
Linear dichroism
Circular dichroism
Polarimetric spectroscopy
Polarization state switching
Microspectrophotometry

ABSTRACT

This study proposes an innovative filter wheel for the multi-channel switching of polarization state. The proposed device enables switching between two orthogonal linear polarization states or two orthogonal circular polarization states to achieve either linear dichroism (LD) or circular dichroism (CD). The filter wheel enables channel switching and orientation rotation with high repeatability. This paper describes in detail the methods used in the alignment of multiple polarizers and quarter-waveplates. In addition, the extinction ratio and retardation, which can be used as indications of polarimetric performance, are measured to a high degree of precision. The apparatus was applied for 6-channel polarization state switching in which three channels were used for multi-spectral broadband polarimetric applications across a range of 400–1600 nm. The remaining three channels were used for multi-wavelength precision polarimetric applications at wavelengths of 457, 532, and 632 nm in the visible range. When installed in a microspectrophotometer, the proposed apparatus can be used in multi-spectral broadband polarimetric spectroscopy as well as multi-wavelength polarimetric imaging applications to achieve LD and CD effects at the micro scale.

1. Introduction

A filter wheel is an optical mechanism commonly used for switching in multiple-channel optical devices. A motorized filter wheel acting as a channel switcher enables the sequential positioning of optical devices within the light path, which makes it ideally suited to the automation of index applications requiring spectral-range selection or optical density attenuation [1,2]. The optical devices used in these applications include multiple filters covering various spectral ranges and multiple neutral-density (ND) filters providing various degrees of attenuation. Motorized filter wheels are widely used in multi-spectral imaging, broadband spectroscopic measurement, and laser applications [3,4]. The motor enables movement in the forward and backward directions with the same functionality in either direction, albeit sequentially reversed. Conventional motorized filter wheels can be used to switch between optical devices but they cannot be used to adjust the orientation. Conventional motorized filter wheels are suitable for most of the optical devices installed in a filter wheel, such as interference and ND filters, due to the fact that they are radially symmetric.

* Corresponding author.
E-mail addresses: cjweng@itrc.narl.org.tw (C-J Weng); L.Wang@kent.ac.uk (L. Wang); chihyenorama@gmail.com (C-Y Chen); daren@itrc.narl.org.tw (D-R Liu); chhwang@itrc.narl.org.tw (C-H Hwang); chang.sw@nsrrc.org.tw (S-W Chang)

https://doi.org/10.1016/j.ijleo.2019.163122
Received 29 April 2019; Accepted 18 July 2019
Available online xxx
0030-4026/

However, the functionality of optical devices used for polarization, such as polarizers and retarders, depends on their orientation. The polarization state of light passing through such devices is altered according to the angle of the transmission axis (polarizers) or the angle of the principle axis (retarders), relative to the original state of polarization. This makes it possible to alter the polarization states by rotating the optical device to change its orientation; however, conventional motorized filter wheels do not allow for this kind of rotation.

Polarization state generators (PSGs) produce arbitrary polarization states and polarization state analyzers (PSAs) are used to determine polarization states. A PSG can be used in conjunction with PSA in the polarimetric analysis of samples. PSGs and PSAs typically have the same configuration but differ in their arrangements. They both include a polarizer and a quarter-waveplate which can be turned to produce an arbitrary polarization state, such as horizontal linear polarization, vertical linear polarization, right-hand circular polarization (RHCP), and left-hand circular polarization (LHCP), as well as other elliptical polarization states. Technological advances have made it possible to employ brighter broadband light sources, such as the high-power lamps, a supercontinuum light source [5], and laser-driven light sources [6]. Broadband light sources covering a spectrum from ultraviolet to infrared light widely used in spectroscopy and multi-wavelength imaging measurements, which are useful for identifying the spectral signature of samples according to absorption, transmission, fluorescence, and resonance. Multi-wavelength imaging is superior to conventional RGB imaging systems in remote sensing, and chemical and biological applications. Polarimetric identification is an important consideration in spectroscopy as well as imaging measurement applications [7–9]. The linear dichroism (LD) and circular dichroism (CD) of anisotropic optical metamaterials can be determined by measuring the polarimetric response of two orthogonal circular polarization states and two orthogonal linear polarization states [10–12]. Polarization devices are the primary elements in any polarimetric system; however, the bandwidth of these devices is limited. As a result, PSAs or PSGs that are configured using polarizers and waveplates are unable to provide coverage across the entire spectral band. For example, the PSAs of Thorlabs based on liquid crystal technology are limited to a bandwidth of just 400 nm [13], which is insufficient for most spectroscopic measurement applications. Achieving broadband coverage from 400 to 1600 nm requires four sets of conventional modules; unfortunately, the integration of these devices can be complicated. Multi-wavelength polarimetric imaging, such as circular dichroism imaging microscopy, is useful in the characterization of chiral optical effects [14]. In a previous study, a motor-driven polarizer was integrated with a tilting compensator driven by a manual actuator to produce two orthogonal circular polarizations at multiple wavelengths and the CD image is scanned continuously across the visible range. However, this configuration does not allow for automatic operations, making the process of measurement somewhat slow. Furthermore, compensating for the limited bandwidth of the polarizer and compensator to deal with visible as well as near-IR requires multiple polarizers and waveplates covering various ranges. At present, the integration of polarization devices is problematic. Conventional motorized filter wheels enable channel switching and the integration of multiple polarization devices; however, they do not allow for adjustments to the orientation.

This study proposes an innovative optical mechanism capable of loading multiple optical polarization devices (e.g. multiple pairs of polarizers and retarders), covering various parts of the spectral range. A single motor-driven apparatus enables the implementation of these devices in the form of a filter wheel while making it possible to rotate the orientation for use as multiple PSGs or PSAs. The resulting device can be viewed as a multi-channel PSG/ PSA for broadband polarimetric spectroscopy and polarimetric imaging applications.

2. Description of optical system

In many industrial applications, a drive unit is integrated with gears to control rotational movements. Unfortunately, most applications involving multiple movements require multiple drive motors. In a conventional system, adjusting the relative angle between polarizers and QWPs in order to change the polarization state would require an additional drive motor and a mechanical transmission system, thereby driving up the size, weight, and cost of the resulting device. In this study, we arranged a number of polarizers/QWP pairs in the form of a circular filter wheel, which are moved into a predetermined position using a single motor drive via mechanical transmission. We developed a novel mechanism that resembles the revolution and rotation of the earth to enable channel switching and orientation adjustment simultaneously [15,[16]]. Fig. 1(a) and 1(b) present the previous and the last schematic illustration of the proposed mechanism respectively, which includes a drive motor, a drive shaft, two unidirectional bearings (UDBs), a plate body, and a drive wheel [16]. The drive motor provides movement in the clockwise as well as counterclockwise directions. The drive shaft is attached at one end to the drive motor, with the other end passing through UDB1 to the other side of the plate body. The drive shaft synchronously rotates the plate body counterclockwise via UDB1 to enable channel switching. The drive shaft also produces clockwise rotation in a drive wheel in contact with passive components positioned on the plate body. These passive components rotate in a clockwise direction to change the orientation of the polarizers. The contact between the drive wheel and passive components is governed by a gear set, which can be adjusted in accordance with the particulars of the application and devices employed. UDB2 is limited in its counterclockwise movement is placed in a position corresponding to the height of the plate body. The position of the plate body can be maintained without clockwise rotation by its contact with the UDB2. The UDB2 is fixed in a position near the plate body, so that it can be rotated clockwise with the plate body.

Operation of the proposed mechanism proceeds through two steps:

Step 1: The motor rotates the drive shaft counterclockwise, which synchronously rotates the plate body moving the passive components, such as multiple polarizers or QWPs, to a predetermined position.

Step 2: The motor rotates the drive shaft clockwise to rotate the drive wheel, which rotates each of the polarizers via a gear set.

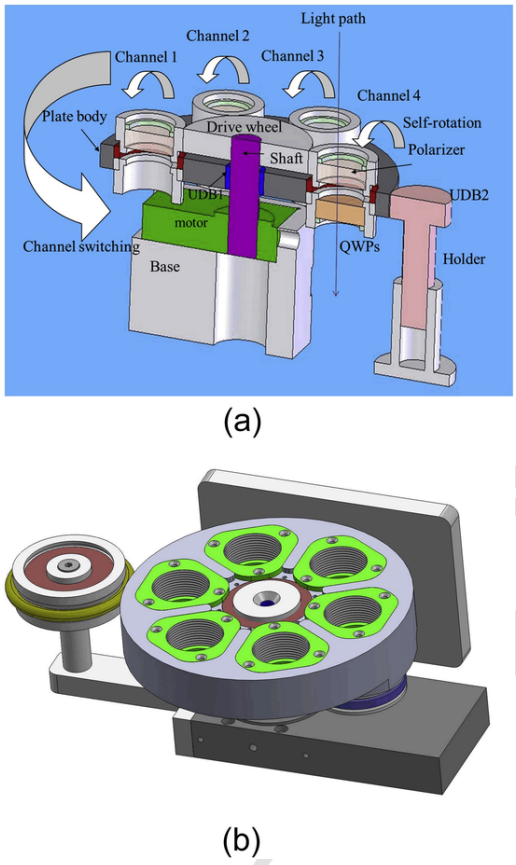

Fig. 1. Schematic diagram showing (a) the previous and (b) the last proposed motorized filter wheels for multi-channel polarization state switching. Channel switching is achieved by operating the motor in the counterclockwise direction in order to rotate the plate body holding the polarizing devices. Orientation adjustment is achieved by reversing the direction of the motor in order to rotate the polarizers in a counterclockwise direction. Unidirectional bearings are used in conjunction with a gear set to differentiate between the two operations.

Rotation of the polarizer to align it with the QWP makes it possible to specify the polarization states according to a predetermined wave band. Rotating the drive shaft counterclockwise (via the motor) moves the plate body to a predetermined position, which switches the channel to the selected polarizer and QWP (with the same optical bandwidth). When rotated in the clockwise direction, the shaft moves the drive wheel (rather than the plate body), which rotates the polarizers. During this operation, the QWPs neither move nor rotate. This novel design enables the functions of channel switching and orientation rotation using a single motor. Fig. 2(a) and 2(b) illustrate the front of the previous and the last mechanism (inverted from Fig. 1). The proposed device includes six channels in the upper plate body to hold six QWPs, as well as six polarizers in the lower plate body. Fig. 3(a) presents a rear-view of the mechanism, showing six polarizers loaded within the surrounding gear sets involved in rotation. The central gear set has 80 teeth and surrounding gear sets each have 40 teeth (gear ratio of 2:1). Using a high-precision Newport 50PP with angular resolution of 0.01°, we achieved a maximum rotation speed of 8°/s, which means that 7.5 s is required for channel-switching and 22.5 s is required to rotate the polarizers into the correct orientation. It's easy to understand that the error of rotation angle for polarization devices rotated by this system is large because this design is based on gear set. The major error is major from the gap of the gear set. To deduce the error of rotation angle, another design based on a high-resolution pulley set and high-precision UDB is proposed as shown in Fig. 3(b). This system is a compact solution for multi-channel polarization state switching. The system performance of both designs will be discussed in the next section.

3. Experiment setup and alignment method

Polarization devices require precise alignment in the azimuth angle: the transmission axis of polarizers, and the principle axis of QWPs. This study used six PSGs loaded on the circular filter wheel as shown in the Fig. 2(b), comprising a polarizer with a waveband-matched QWP to enable the arbitrary selection of polarization state (linear, circular, or elliptical), simply by rotating the polarizer while maintaining the QWP in a stationary position. Achieving a precise polarization state requires precise alignment between the transmission axis of the polarizer and the principal axis of the QWP. This study employed sheet polarizers and thin achromatic QWPs to prevent aberration, which would otherwise distort the image and decrease the signal-to-noise ratio in imaging and spectroscopic measurements. The characteristics of the polarizers and QWPs used in the circular filter wheel are listed in Table 1.

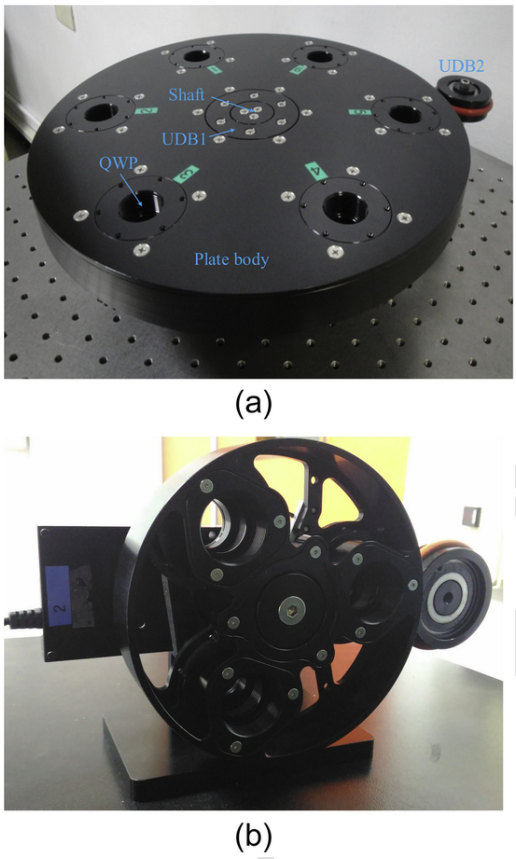

Fig. 2. Top-view of (a) the previous and (b) the last proposed motorized filter wheels. Rotating the drive wheel in a counterclockwise direction causes the plate body to rotate, thereby moving a new polarizer into position. The light path is from bottom to top; therefore, the QWPs are positioned in the upper plate body with polarizers in the lower plate body.

To enable polarimetric spectroscopy covering a waveband from 400 to 1600 nm, we matched three sheet polarizers with three achromatic QWPs for three wavebands: 400 to 700 nm (VIS), 700 to 1000 nm (NIR1), and 1000 to 1600 nm (NIR2). Most conventional sheet polarizers have a high extinction ratio and wide bandwidth. This study used three sheet polarizers manufactured by Thorlabs: the LPVISE100 series (for VIS), LPVIS series (for NIR1), and LPNIR (for NIR2), which were designated as channels 1, 2, and 3, respectively. In contrast, bandwidth of most conventional achromatic QWPs is narrow. We conducted a survey of conventional QWP products, the retardation curves of which are presented in Fig. 4. The bandwidth at short wavelengths is narrower than at long wavelengths. To match the polarizers, we selected Newport 10RP54-1 for VIS, 10RP54-2 for NIR1, and 10RP54-3 for NIR2. These products are achromatic zero-order quartz-MgF2 waveplates with retardance of approximately $0.25\lambda \pm 0.015\lambda$across the VIS range and $0.25\lambda \pm 0.005\lambda$ for NIR1 and NIR2. The variations in retardance at VIS wavelengths greatly exceeded those in the NIR1 and NIR2 ranges due to the dispersal characteristics of the material.

Three LPVISE100 sheet polarizers with the same bandwidth (400–700 nm) were installed within channels 4, 5, and 6 in the lower plate body. QWPs are the components crucial to the precision of polarization states. Zero-order quartz QWPs are temperature-insensitive phase retarders ideally suited to precision polarimetric imaging applications. We installed true zero-order quartz QWPs with center wavelengths of 457 nm (series#WPH10M-457), 532 nm (series#WPH10M-532), and 632 nm (series#WPH10M-632) manufactured by Thorlabs in channels 4, 5, and 6 in the upper plate body. Sheet polarizers can be combined with QWPs to produce precise polarimetric images with the CD response of the sample in the red (R), green (G), and blue (B) wavebands. As shown in Fig. 5, we installed the proposed apparatus in a broadband microspectrophotometer (MSP) to evaluate the performance of the system [17,[18]]. An MSP with CCD and spectrometer was modified from a Zeiss axio D2 upright microscope. Automatic operation of the apparatus was enabled using a PC equipped with LabVIEW software. A Glan-Taylor type broadband polarizer (CVI PTYL) was installed at the top of the microscope to facilitate alignment of the apparatus.

Malus's law was used to align the transmission axis of the sheet polarizers. The transmission intensity, denoted as I can be expressed as follows:

$$I = I_0 \cos^2\theta, \tag{1}$$

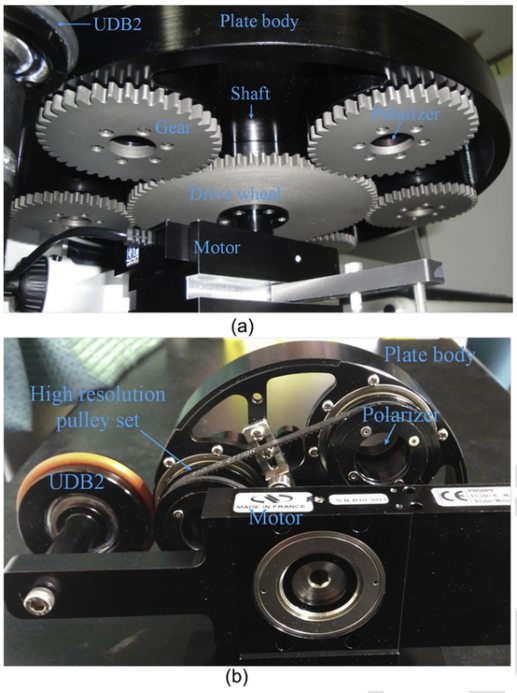

Fig. 3. Rear-view of motorized filter wheel. Rotating the drive wheel in a clockwise direction causes the rotation of the polarizers, UDB2 is used to prevent the plate body from rotating when the motor drives the shaft in a clockwise direction: (a) the first design based on gear set, (b) the later design based on a high-resolution pulley set and high-precision UDB.

Table 1
Wavebands and series numbers of polarizers and QWPs installed in circular filter wheel. Channel 1, Channel 2, and Channel 3 are for broadband multi-spectral application whereas Channel 4, Channel 5, and Channel 6 are for multi-wavelength applications.

Channel # devices	Channel 1 VIS 400-700 nm	Channel 2 NIR1 700-1000nm	Channel 3 NIR2 1000-1600nm	Channel 4 Blue band 457nm	Channel 5 Green band 532nm	Channel 6 Red band 632nm
Polarizers	LPVISE100	10LP-VIS-B	LPNIR-2	LPVISE100	LPVISE100	LPVISE100
QWPs	10RP54-1 achromatic quartz-MgF_2	10RP54-2 achromatic quartz-MgF_2	10RP54-3 achromatic quartz-MgF_2	WPH10M-457 zero-order quartz	WPH10M-532 zero-order quartz	WPH10M-632 zero-order quartz

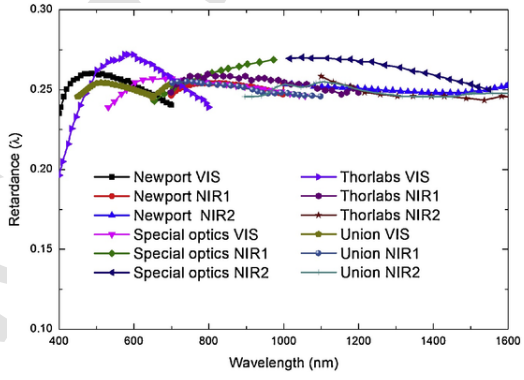

Fig. 4. Retardation curves of commercial QWPs. Covering a range from 400 to 1600 nm required three QWPs: VIS, NIR1, and NIR2.

where θ is the relative angle between the polarizer and analyzer and I_0 is the intensity when the axis of transmission of the polarizer is parallel to that of the analyzer. All of the polarizers manually rotated until transmitted light reached the maximal intensity, which occurred when the x-axis was at an angle of 0° relative to the transmission axis of the analyzer, thereby resulting in horizontal linear polarization. The motorized mechanism within the apparatus was then used to switch sequentially to the following polarizer in

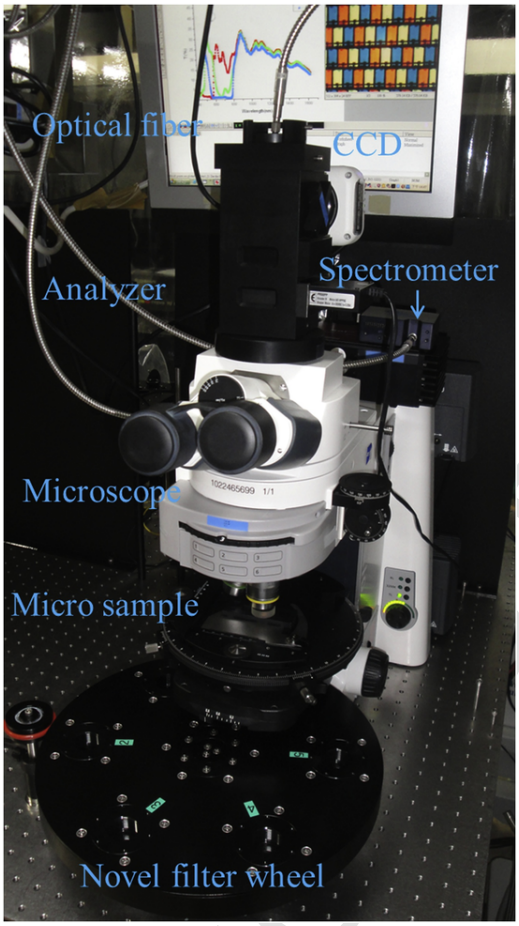

Fig. 5. Proposed filter wheel installed in a broadband microspectrophotometer. The light path proceeds vertically from the bottom to determine the transmission mode with light passing through the apparatus, micro sample, the objective lens, the analyzer, and the spectrometer via fiber couplers.

the wheel, which was then calibrated by hand to the same angle of 0°. The motor was then used to rotate the polarizers to the point at which the orientation angles along the transmission axes of the six polarizers were coherent. Following the alignment of the polarizers, any angle could be easily achieved simply by stipulating the LabVIEW the degree of rotation of the motor (e.g., 0°, ±45°, or ±90°) for polarimetric measurement. For example, the LD effect of the sample could be obtained by measuring the orthogonal linear polarization without the need to install QWPs. Absorption horizontal polarization is denoted as A_x. The apparatus can rotate 90° when all three polarizers are in a state of vertical polarization. The absorption for samples is denoted as A_y in the vertical polarization. LD can be expressed as follows [19]:

$$LD = A_x - A_y. \tag{2}$$

The principal axes of the six QWPs also require precise alignment. We began by setting the transmission axis of the analyzer to 90° and the transmission axes of the polarizers to 0°, such that almost no light would be able to penetrate between them. The QWPs were then manually rotated until the maximum light transmission was reached, at which point the principal axes of the QWPs were approximately 45°; i.e., the orientation pertaining to circular polarization (with the polarizers still oriented at 0°). Unfortunately, obtaining precise measurements of the principal axis orientation angle while simultaneously determining the degree of retardation can be difficult. We adopted the three-step method proposed by Safrani [20] in which the analyzer is rotated to three successive positions (0°, 45°, and 90°) with respect to the x-axis of the polarizer. The intensities at 0°, 45°, and 90° are denoted as I_{0°, I_{45°, and I_{90°, respectively. Angles φ and δ represent the principal axis orientation angle with respect to the x-axis and retardation, respectively.

$$\varphi = \frac{1}{2} Cot^{-1}\left\{\frac{1}{2}\left[1 - \frac{2I_{45^\circ} - I_{90^\circ}}{I_{0^\circ}}\right]\right\}, \tag{3}$$

with

$$\delta = \mathrm{Cos}^{-1}\left\{1 - \frac{2}{I_{0^\circ}+I_{90^\circ}} \times \left\{I_{0^\circ} + \frac{1}{4I_{0^\circ}}[I_{0^\circ} - 2I_{45^\circ} + I_{90^\circ}]^2\right\}\right\}. \quad (4)$$

This method makes it possible to align and measure the QWPs with a high degree of precision. To achieve circular polarization for CD measurement, we set the fast principal axis orientation angle of the QWP to 45° with respect to the x-axis of the polarizer. The RHCP and LHCP are created by setting the transmission axes of the polarizers at 0° and 90° while maintaining the QWPs at 45°. The difference in intensity between RHCP and LHCP in spectroscopic imaging represents the effect of CD. The absorption of the sample associated with RHCP polarization is denoted as A_{RHCP}. We then rotated the apparatus 90°, such that the three polarizers maintained vertical polarization with the QWPs remaining at 45° with respect to the x-axis. The absorption of the sample associated with LHCP is denoted as A_{LHCP}. Circular dichroism can be expressed as

$$CD = A_{RHCP} - A_{LHCP}. \quad (5)$$

In this manner, it is possible to obtain polarimetric measurements in broadband spectroscopy and multi-wavelength images, such as LD and CD. This proposed filter wheel can also be installed in a microscope as a polarimetric MSP for the examination of samples with CD and LD characteristics.

4. Experiment results and discussion

To characterize the mechanical performance of the apparatus, we installed a HeNe laser, six LPVISE100 polarizers, and a polarimeter (Meadowlark Optics) to measure the degree of accuracy that could be maintained after repeated channel switching and orientation rotation [21]. The alignment of the six polarizers was initially set at 0°. The resolution of the polarimeter with regard to rotation was 0.01°. The transmission axis angle of the polarizer was measured for angle variation after Channel 1 repeated the circuit in the first design based on gear set as illustrated in the Fig. 3(a). Fig. 6(a) shows the repeatability for the same channel, which was cycled repeatedly. The variation in the experiment results was ± 0.2°. In the 60° sequential rotation of the apparatus (i.e., sufficient for switching to the next adjacent channel), the repeatability was approximately ± 0.2°. The degree of variation was the same for same-channel switching as for adjacent-channel switching. This can be attributed primarily to the gaps in the UDB. The same

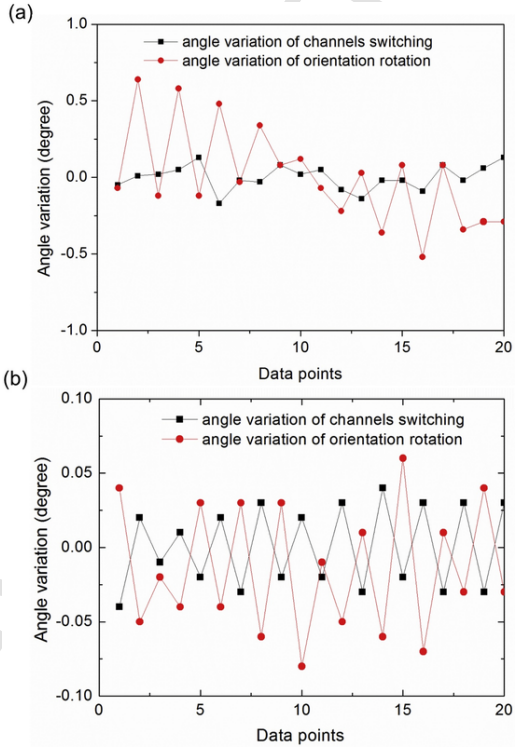

Fig. 6. Geometric variations associated with channel switching and orientation rotation. The variation associated with orientation rotation exceeds that of channel switching due to the gaps between cogs in the gear sets: (a) the first design based on gear set, (b) the later design based on a high-resolution pulley set and high-precision UDB.

method was used to evaluate the repeatability of orientation rotation in channel 1. As shown in Fig. 6(a), the transmission angle of the polarizers after each cycle of orientation rotation was ± 0.7°, due primarily to gaps between the cogs in the mechanical gearing mechanism. This unacceptable degree of variation could no doubt be corrected through the use of high-precision pulleys rather than gears. In the later design as shown in the Fig. 3(b), the repeatability for both of channel switching and orientation rotation is significantly reduced to be approximately ± 0.1° as shown in the Fig. 6(b). The amount of error associated with channel switching and orientation rotation was sufficiently small to be disregarded.

The proposed novel filter wheel can create any polarization during a time sequential slot. Before placing the QWPs, the linear polarization with any azimuthal angle can be produced by selecting the function of orientation rotation with the motor driving after calibration of transmission axis of the polarizer in the Channel 1. The linear polarization states with 0° /45° / 90° are produced for the illustration as shown in the Fig. 7. The results were measured from the conventional polarimeter. Mechanical errors shifted the transmission axis of the polarizer by 0.27° from the initial horizontal (0°) as shown in the Fig. 7(a). When the polarizer was subsequently rotated to 90° (vertical polarization), the measured angle was actually 89.89°, i.e., a shift of 0.11°. When the polarizer was subsequently rotated to 45°, the measured angle was actually 45.01°, i.e., a shift of 0.01°. Therefore, the proposed novel filter wheel for multi-channel polarization state switching has the characteristics of high resolution and accuracy. It is enough to be applied in the applications of broadband polarimetric microspectrophotometry.

The extinction ratio and the retardation were used to determine the performance of the apparatus with regard to multi-spectral broadband polarimetric measurement. The polarizers and QWPs were installed as shown in Table 1. Fig. 8 presents the experiment results pertaining to the extinction ratio in two orthogonal linear polarization states, from Channel 1 to Channel 3, as an indication of the performance of the polarizers. In the three curves, the extinction ratio was between 18 and 30 dB in the VIS range just above 35 dB in NIR1 and NIR2.

After placing the QWPs in the upper plate body, the other elliptical polarization states can be produced by combining polarizers and QWPs via motor forward driving the orientation rotation of polarizers. Therefore, this system is a time-sequential complete polarimeter. It's possible to achieve the usual complete measurement of the Stokes parameters [22]. We experimentally measured the retardation of three narrow-band zero-order QWPs (Channels 4 to 6) using a three-step method as an indication of the performance of the QWPs. The red band (632-nm) zero-order QWP in Channel 6 underwent three measurements of intensity, as shown in Fig. 9. The three curves intersect at 632 nm, at which point the intensity values were very close, i.e., similar to those associated with a

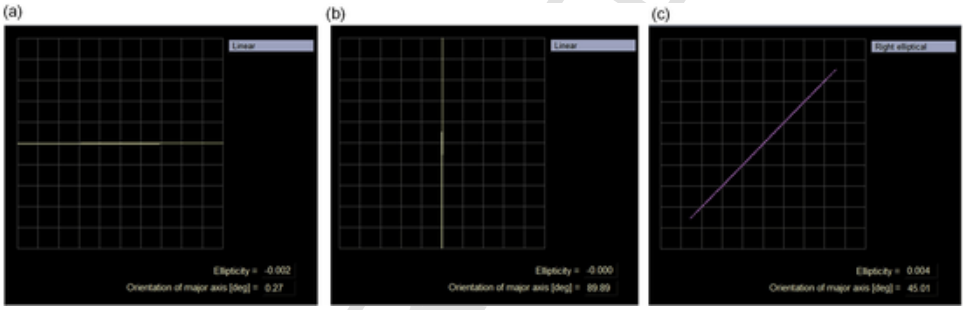

Fig. 7. Switching of two orthogonal linear polarization states at 632 nm: (a) horizontal (0°) linear polarization, (b) vertical (90°) linear polarization, and (c) 45° linear polarization.

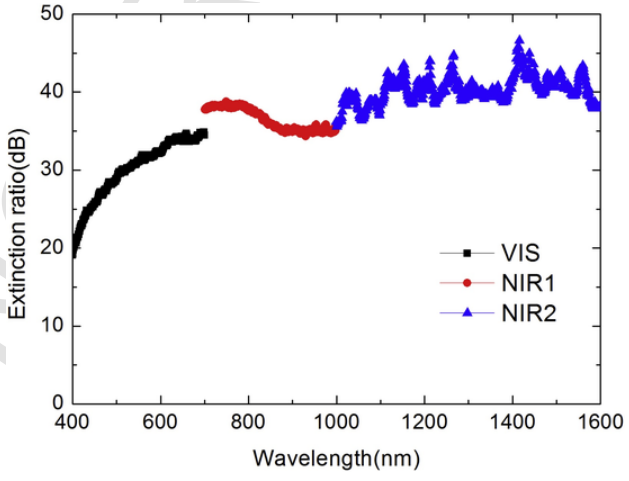

Fig. 8. Extinction ratios associated with two states of orthogonal linear polarization in three ranges: VIS, NIR1, and NIR2.

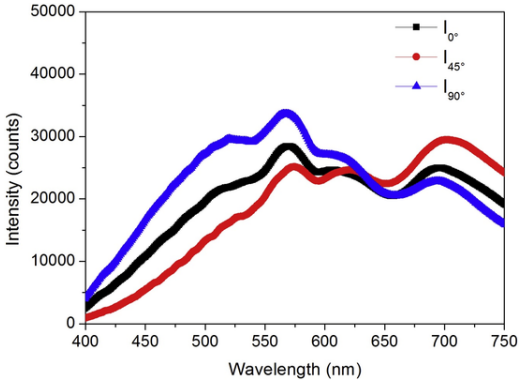

Fig. 9. Three intensity curves versus wavelength: I0°, I45°, and I90°. Close to the quarter-wave at 632 nm the three curves resemble each other.

quarter-wave. The principal axis orientation angle and retardation of zero-order QWPs can be calculated using (3) and (4), respectively. First, the orientation angle of the principal axis was calculated as shown in Fig. 10(a). The curve presents a small ripple in that range of measurement range due to the fact that the zero-order QWPs are thin and the two sides are highly parallel, such that the light beams from two surfaces are susceptible to interference with each other. Avoiding this problem requires that the QWPs be installed with a slight tilt and that an AR coating be applied to their surfaces. Narrow bandpass filters with a center wavelength of 632 nm can also be inserted in the optical path to exclude light of other wavelengths. Fig. 10(b) presents the measured retardance curve and the curve included in the Thorlabs specifications. The retardation presented by the zero-order QWPs is linearly inversely proportional to the wavelength. Nonetheless, the experimental results present a small ripple in the measured range due to interference. This simple three-step method for the measurement of retardation is highly accurate; however, the measurement of the principal axis orientation angle provides greater accuracy.

Two orthogonal circular polarization states at 632 nm can be produced by altering the orientation of polarization. We employed a polarimeter with a HeNe laser to monitor the state of polarization with the principal axis set at 45° and the angle of the transmission axis of the polarizer (Channel) 6 set to 0° and 90, i.e., polarization states of RHCP and LHCP, respectively. As shown in Fig. 11,

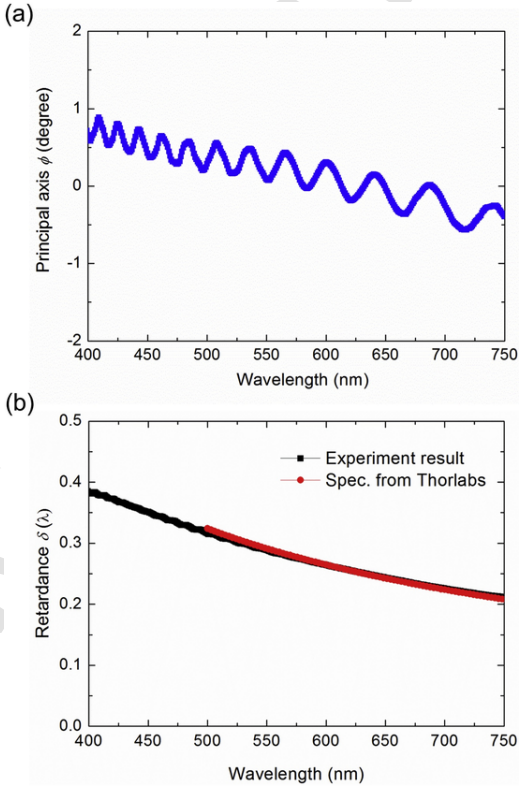

Fig. 10. (a) Orientation angle of principal axis versus wavelength in degrees; (b) Spectral retardation versus wavelength in waves for both measurement and specification.

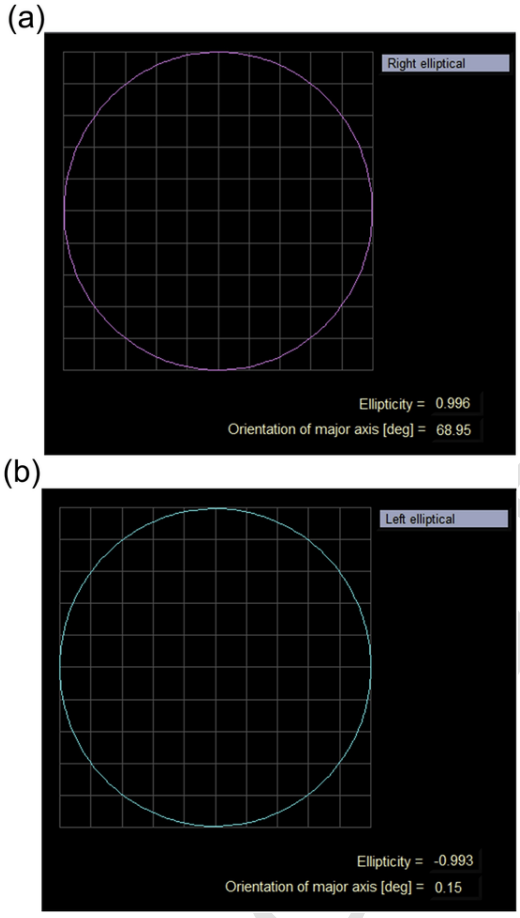

Fig. 11. Two orthogonal circular polarization states at 632 nm (a) right-hand circular polarization, and (b) left-hand circular polarization.

the ellipticity of RHCP was 0.996 and ellipticity of LHCP was 0.993, both of which are indicative of nearly perfect circular polarization.

The two QWPs covering the green and blue bands were measured using the same method. Fig. 12 presents the retardance curve of the three narrow-band QWPs, indicating retardance equal to a quarter of the wavelength in the design. The accuracy of the multi-wavelength retardance was compared to the specifications provided by Thorlabs. The retardance value in the red band in Channel 6 is 0.2485 λ at 632 nm, whereas the original specification is 0.2511 λ, representing a discrepancy of 0.0026 λ. The retardance value in the green band in Channel 5 is 0.2508 λ, whereas the original specification is 0.2494 λ, representing a discrepancy of 0.0014 λ. The retardance value in the blue band in Channel 4 is 0.2465 λ, whereas the original specification is 0.2500 λ, representing a discrepancy of 0.0035 λ. These results illustrate the high degree of accuracy in the visible range in Channel 4 to Channel 6.

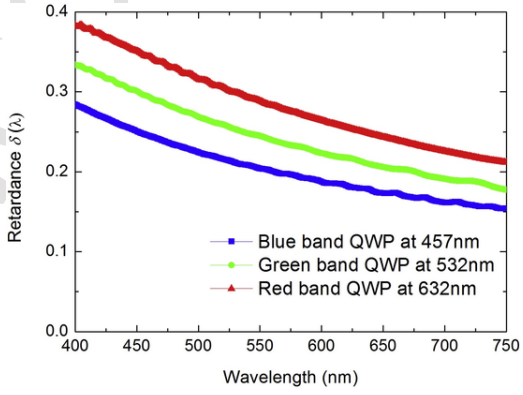

Fig. 12. Spectral retardation versus wavelength associated with zero-order quartz QWPs in the VIS range.

Compared with the specifications from Newport, as shown in Fig. 13, the VIS curve varied more noticeably than the other two curves. This phenomenon can be attributed to the dispersity of the QWP material in the VIS range. The NIR1 and NIR2 curves are flatter, indicating adequate achromatic compensation. Retardation across the entire VIS band was approximately 0.25λ ± 0.02λ, whereas retardation in NIR1 and NIR2 was approximately 0.25λ ± 0.01λ. Compared to the specifications from Newport, the difference between the measured results and the designed value was less than 0.02λ across the entire broadband bandwidth from 400 to 1600 nm. The retardance values measured for the QWPs in Channels 1 to 6 are listed in Table 2. Our results demonstrate the precision in the alignment of the multi-QWPs installed in the apparatus, with the error attributed to the imperfect collimation of the broadband light source within the microscope and mechanical variations associated with the operation of the proposed apparatus. Measurement error could be further reduced by applying a highly collimated light source, such as a supercontinuum light source, whereas the mechanical errors could be remedied through the substitution of gears for high-resolution pulley set.

5. Conclusion

Channel switching and orientation adjustment are indispensable in multi-channel polarization state switching, particularly when applied to multi-spectral polarimetric spectroscopy or multi-wavelength polarimetric imaging applications. Conventional motorized filter wheels do not provide a function by which to align the azimuth angle or orientation angle of polarizing filters. This paper reports an innovative filter wheel that uses a precision motor to facilitate the application of multi-channel polarization devices. The device can be loaded with six pairs of polarizers and QWPs of various wavebands to provide six PSGs in discrete channels. The proposed device requires only one precision motor to provide channel switching as well as orientation rotation. The proposed device enables channel switching with repeatability of approximately ± 0.1°. Rotating the polarizers while the QWPs remain stationary make it possible to realize two linear orthogonal polarization states or two circular orthogonal polarization states for LD and CD measurement with repeatability of approximately ± 0.1°. The proposed apparatus is applicable in multi-spectral broadband polarimetric spectroscopy covering a range of 400–1600 nm through the use of three sheet polarizers and three achromatic zero-order quartz-MgF2 QWPs. The proposed instrument would be useful in fields such as chiral metamaterials, plasmonics, micro polarization optics, green optics, and bio optics. Multi-band PSAs can also be integrated within the apparatus.

Acknowledgment

The authors would like to thank Mr. Shian-Wen Chang and Mr. Gang-Hong Fan for their technical help. This work was sponsored in part by the Ministry of Science and Technology, Taiwan, R.O.C. under contract number MOST 103-2622-E-492-019-CC3.

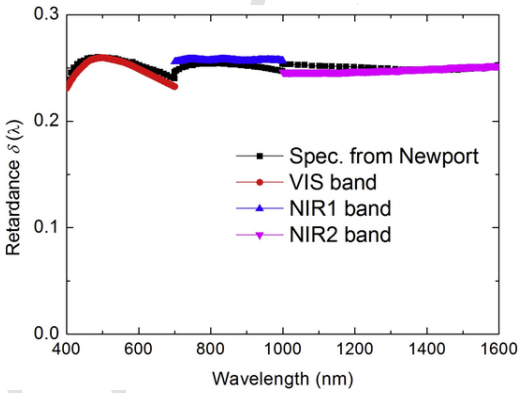

Fig. 13. Experiment results indicating degree of retardation from three broadband achromatic zero-order QWPs with the Newport specifications as a baseline reference.

Table 2
Comparison of experiment results and reference values in six channels.

Channe1 # Comparison	Channel 1 VIS band	Channel 2 NIR1 band	Channel 3 NIR2 band	Channel 4 Blue band	Channel 5 Green band	Channel 6 Red band
Specification	0.25 ± 0.015 λ	0.25 ± 0.01 λ	0.25 ± 0.005 λ	0.2500 λ	0.2494 λ	0.2511 λ
Experimental results	0.25 ± 0.02 λ	0.25 ± 0.01 λ	0.25 ± 0.005 λ	0.2465 λ	0.2508 λ	0.2485 λ

References

[1] J. Brauers, et al., Geometric calibration of lens and filter distortions for multispectral filter-wheel cameras, IEEE Trans. Image Process. 20 (2011) 496–505.
[2] J.H. Bowles, et al., Airborne system for multispectral, multiangle polarimetric imaging, Appl. Opt. 54 (31) (2015) F256–F267.
[3] J.C. Simon, et al., Combining multispectral polarized light imaging and confocal microscopy for localization of nonmelanoma skin cancer, Lasers in Dentistry XXIV. Vol. 10473. International Society for Optics and Photonics 10473, 2018 1047305.
[4] C.J. Weng, et al., Exploiting the image of the surface reflectivity to measure refractive index profiling for various optical fibers, Opt. Express 23 (9) (2015) 11755–11762.
[5] C.L. Thomsen, et al., New horizons for supercontinuum light sources: from UV to mid-IR, Proc. SPIE. Int. Soc. Opt. Eng. 8637 (2013) 86370T.
[6] S. Horne, et al., A novel high-brightness broadband light-source technology from the VUV to the IR, Proc. SPIE. Int. Soc. Opt. Eng. 7680 (2010) 76800L.
[7] G.C. Giakos, Multifusion multispectral lightwave polarimetric detection principles and systems, IEEE Trans. Instrum. Meas. 55 (6) (2006) 1904–1911.
[8] M. Yu, et al., Multispectral Stokes imaging polarimetry based on color CCD, IEEE Photonics J. 8 (5) (2016) 1–10.
[9] B. Baumann, Polarization sensitive optical coherence tomography: a review of technology and applications, Appl. Sci. 7 (5) (2017) 474.
[10] W.T. Chen, et al., Manipulation of multidimensional plasmonic spectra for information storage, Appl. Phys. Lett. 98 (2011) 171106.
[11] M. Ren1, et al., Giant nonlinear optical activity in a plasmonic metamaterial, Nat. Commun. 3 (2012) 833.
[12] M.R. Shcherbakov, et al., Plasmonic enhancement of linear birefringence and linear dichroism in anisotropic optical metamaterials, JETP Lett. 90 (2009) 433.
[13] Thorlabs specification sheet of Polarization Instrumentation, http://thorlabs.com.
[14] K. Claborn, et al., Circular dichroism imaging microscopy: application to enantiomorphous twinning in biaxial crystals of 1,8-dihydroxyanthraquinone, J. Am. Chem. Soc. 125 (48) (2003) 14825–14831.
[15] S. W. Chang et al., "Mechanism with component position adjusting functions," United State Patent, US 2013/0045830A1 (2013).
[16] C.J. Weng, et al., Compact motorized circular wheel of polarization optics for ultrabroadband polarization state generation, Proc. SPIE. Int. Soc. Opt. Eng. 8487 (2012) 848705.
[17] C.J. Weng, et al., Broadband microspectrophotometer with tablet PC control, IEEE International Instrumentation and Measurement Technology Conference, 2012, pp. 2434–2439.
[18] C.J. Weng, et al., Developing a microspectrophotometer to measure the dependence of broadband refractive indices on Ge-doped concentrations in GRIN rods, Opt. Express 23 (24) (2015) 30815.
[19] E. Hecht, Optics, Addison Wesley, New York, 2002.
[20] A. Safrani, et al., Spectropolarimetric method for optic axis, retardation, and birefringence dispersion measurement, Opt. Eng. 48 (5) (2009) 053601-1~053601-10.
[21] Meadowlark specification sheet of polarimeter, http://www.meadowlark.com.
[22] A. Peinado, et al., Optimization and performance criteria of a Stokes polarimeter based on two variable retarders, Opt. Express 18 (10) (2010) 9815–9830.